Am J Cancer Res 2021;11(2):350-369
www.ajcr.us /ISSN:2156-6976/ajcr0122297

Original Article

Adamantane-linked isothiourea derivatives suppress the growth of experimental hepatocellular carcinoma *via* inhibition of TLR4-MyD88-NF-κB signaling

Hanan M Hassan[1], Lamya H Al-Wahaibi[2], George SG Shehatou[1,3], Ali A El-Emam[4]

[1]Department of Pharmacology and Biochemistry, Faculty of Pharmacy, Delta University for Science and Technology, International Costal Road, Gamasa 11152, Mansoura, Egypt; [2]Department of Chemistry, College of Sciences, Princess Nourah bint Abdulrahman University, Riyadh 11671, Saudi Arabia; [3]Department of Pharmacology and Toxicology, Faculty of Pharmacy, Mansoura University, Mansoura 35516, Egypt; [4]Department of Medicinal Chemistry, Faculty of Pharmacy, Mansoura University, Mansoura 35516, Egypt

Received September 13, 2020; Accepted December 11, 2020; Epub February 1, 2021; Published February 15, 2021

Abstract: In this study, *in vitro* cytotoxic effects of seven adamantyl isothiourea derivatives were evaluated against five human tumor cell lines using the MTT assay. Compounds 5 and 6 were found to be the most active derivatives particularly against hepatocellular carcinoma (HCC). To decipher the potential mechanisms involved, *in vivo* studies were conducted in rats by inducing HCC *via* chronic thioacetamide (TAA) administration (200 mg/kg, i.p., twice weekly) for 16 weeks. Compounds 5 and 6 were administered to HCC rats, at a dose of 10 mg/kg/day, for further 2 weeks. *In vitro* and *in vivo* antitumor activities of compounds 5 and 6 were compared to those of the anticancer drug doxorubicin (DOXO). In the HCC rat model, compounds 5 and 6 significantly reduced serum levels of ALT, AST with ALP and α-fetoprotein. H & E and Masson trichrome staining revealed that both compounds suppressed hepatocyte tumorigenesis and diminished fibrosis, inflammation and other histopathological alterations. Mechanistically, compounds 5 and 6 markedly decreased protein expression levels of α-SMA, sEH, p-NF-κB p65, TLR4, MyD88, TRAF-6, TNF-α, IL-1β and TGF-β1, whereas they increased caspase-3 expression in liver tissues of HCC rats. In most analyses, the effects of compound 6 were more comparable to DOXO than compound 5. These findings suggested that the compounds 5 and 6 displayed *in vitro* and *in vivo* cytotoxic potential against HCC, probably *via* inhibition of TLR4-MyD88-NF-κB signaling.

Keywords: Adamantyl isothiourea, hepatocellular carcinoma, epoxide hydrolase, TLR4, MyD88, NF-κB

Introduction

Hepatocellular carcinoma (HCC) is among the most common cancer types, accounting for 8.2% of cancer-related death worldwide [1]. Several etiologies of chronic liver inflammation, including viral hepatitis B (HBV) and C (HCV) infection, excessive alcohol intake and non-alcoholic fatty liver disease, inevitably lead to liver cirrhosis, the major risk factor for the development of HCC [2]. Multiple molecular pathways contribute to the initiation and progression of HCC [3]. Of these, Toll-like receptor 4 (TLR4)/the myeloid differentiation primary response 88 (MyD88)/nuclear factor-κB (NF-κB) cascade has been suggested to be implicated in inducing liver inflammation and promoting progression to cirrhosis and HCC [4-7]. TLR4 is expressed in different liver cell types, including Kupffer cells, hepatocytes and stellate cells and functions as a receptor for lipopolysaccharide (LPS) from intestinal microbiota [4, 8]. LPS can bind and activate TLR4, recruiting MyD88 that triggers the downstream adapter protein tumor necrosis factor (TNF) receptor-associated factor 6 (TRAF-6), which activates NF-κB, resulting in the production of proinflammatory cytokines [8]. Overexpression of TLR4 was detected in livers from HBV and HCV patients and HCC tissues [6, 9, 10]. On the other hand, TLR4-deficient mice showed less fibrosis in experimental fibrosis models, indicating a role of TLR4 in hepatic fibrogenesis [7]. Moreover, deficiency of TLR4 and MyD88 in mice resulted in reduced incidence, number and size of diethylnitrosamine (DEN)-induced HCC tumors [11].

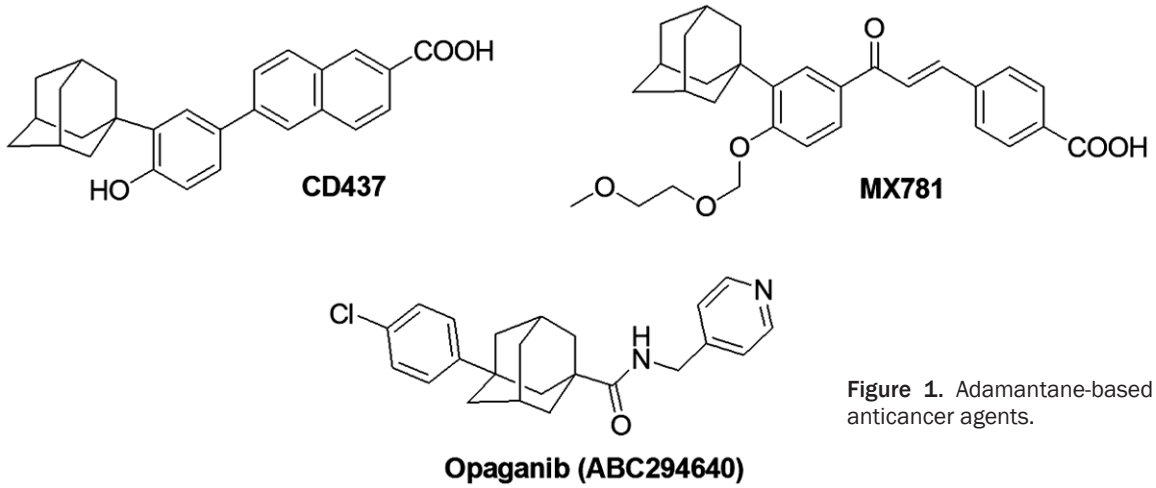

Figure 1. Adamantane-based anticancer agents.

The adamantane nucleus is an established pharmacophore in numerous chemotherapeutic agents [12-14]. The adamantane-based analogues exhibited significant antiviral activity against influenza A viruses [15, 16], human immunodeficiency viruses [17, 18] and herpes simplex viruses [19].

Anticancer activity was reported for some adamantane derivatives (**Figure 1**). The synthetic retinoid adamantane derivative CD437 was discovered as a potent inducer of apoptosis in human primary tumor types, including ovarian cancer, non-small cell lung cancer, leukemia, breast cancer and squamous cell carcinoma [20, 21]. The adamantyl arotinoid chalcone derivative MX781 was also developed as anticancer acting via inhibition of IκB kinase [22, 23]. Opaganib (ABC294640) is a recently approved anticancer drug for the treatment of patients with advanced solid tumors [24, 25].

Interestingly, previous research has shown that adamantane derivatives containing an isothiourea moiety can inhibit soluble epoxide hydrolase (sEH) enzyme [26-28]. Inhibition of sEH is potentially associated with attenuation of inflammation [29]. Pharmacological inhibition of sEH reduced liver fibrosis in carbon tetrachloride-treated rats [30]. A combination of sEH inhibitor and cyclooxygenase-2 inhibitor suppressed primary lung tumor in mice [31].

In a previous study [32], we reported the synthesis and potent broad spectrum antibacterial activity of series of adamantyl isothiourea derivatives namely 4-arylmethyl (*Z*)-*N*'-(adamantan-1-yl)-4-phenylpiperazine-1-carbothioimidates (**Figure 2**, compounds 1-4) and arylmethyl (*Z*)-*N*'-(adamantan-1-yl)-morpholine-4-carbothioimidates 5-7 (**Figure 2**, compounds 5-7). Based on the pronounced anticancer activities of adamantane derivatives [20-25] and marked chemotherapeutic properties of isothiourea derivatives [32-37], it was of interest to study the anticancer activity of adamantane-linked isothiourea derivatives 1-7. The *in vitro* cytotoxic activity of compounds 1-7 was assessed towards five human tumor cell lines, and the *in vivo* activity was further evaluated for the highly active compounds 5 and 6 against HCC in rats.

Materials and methods

Chemicals and reagents

Adamantane isothiourea derivatives 1-7 were prepared following the previously described procedure [32]. Doxorubicin (DOXO), thioacetamide (TAA), dimethyl sulfoxide (DMSO), 3-(4,5-dimethylthiazol-2-yl)-2,5-diphenyl-tetrazolium bromide (MTT) and RPMI-1640 medium were purchased from Sigma Aldrich Chemical Co. (St. Louis, MO, USA). Fetal bovine serum (FBS), penicillin sodium and streptomycin sulfate were obtained from Gibco Ltd (Paisley, UK). All other chemicals were of the analytical reagent grades.

Cell lines

Five human tumor cell lines, namely prostate cancer (PC-3), colorectal carcinoma (HCT-116), breast cancer (MCF-7), human cervical epithelioid carcinoma (Hela) and HCC (Hep-G2) were

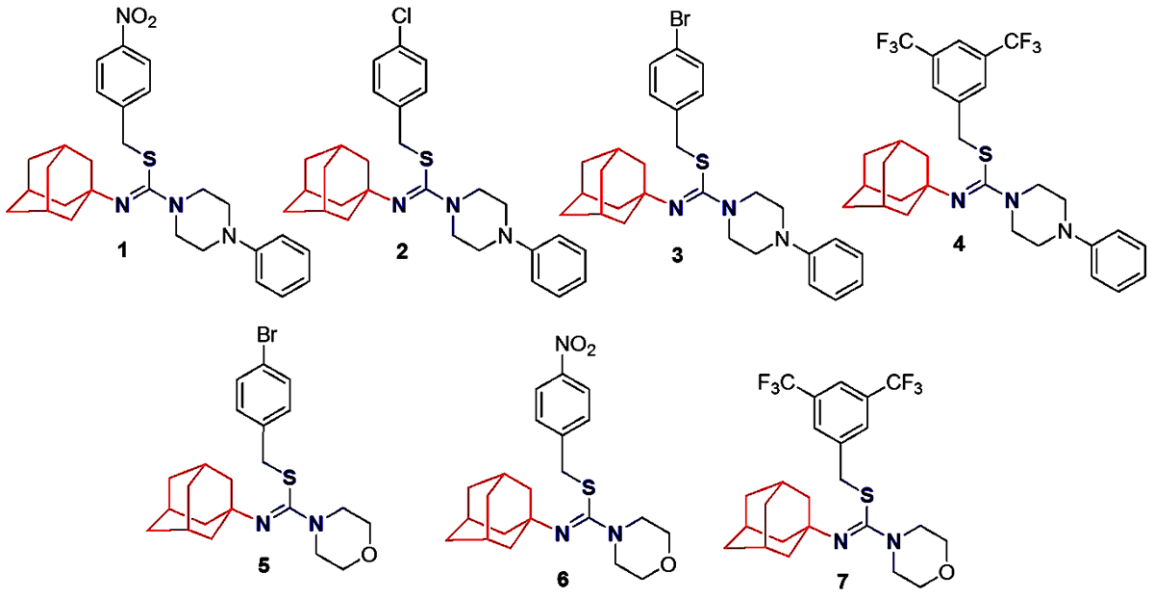

Figure 2. The structures of the investigated adamantane-linked isothiourea derivatives. The red and blue moieties denote the adamantane and isothiourea fragments, respectively.

obtained from American Type Culture Collection (ATCC) via Holding company for biological products and vaccines (VACSERA, Cairo, Egypt). Cells were cultured in RPMI-1640 medium, containing 10% FBS, 100 U/mL penicillin and 100 µg/mL streptomycin, and incubated in a 5% CO_2 humidified atmosphere at 37°C.

In vitro MTT cytotoxicity assay

The cytotoxic effects of compounds 1-7 on human cancer cell viability were assessed using the MTT assay [38, 39]. Briefly, PC-3, HCT-116, MCF-7, Hela and Hep-G2 cells were grown at ~70-80% confluence, dispersed by trypsin and then plated at a density of 1.0×10^4 cells/well in 96-well plates for 48 hours. The cells were then treated with different concentrations of test compounds and further incubated for 24 hours. After the incubation period, 20 µL of MTT solution (5 mg/mL) was added into each well and plates were incubated for 4 hours at 37°C. The supernatants were then removed and 100 µL of DMSO was added into each well to dissolve the formed purple formazan color. The absorbance at 570 nm were determined using ELx800 Microplate Reader (Biotek, Winooski, VT, USA). The relative cell viability was calculated, as follows:

$$\text{Cell viability (\%)} = \frac{A_{570} \text{ of compound - containing wells}}{A_{570} \text{ of DMSO - containing control wells}} \times 100$$

Three independent experiments were performed in duplicate were conducted to calculate the half maximal inhibitory concentration (IC_{50}) values.

Animals

Male Sprague-Dawley rats (180-200 g) were obtained from VACSERA. Animals were maintained under standard laboratory conditions (temperature: 23 ± 2°C, regular 12 hours light-dark cycle, free access to food and water). The animals were permitted to acclimatize to the laboratory environment for 10 days before the start of the experiment. The Research Ethics Committee of the Faculty of Pharmacy, Delta University for Sciences and Technology approved the experimental protocols (FPDU 16/2020), which were in accordance with National Institute of Health guidelines for laboratory animal care (NIH publication No. 85-23, revised 2011).

Thioacetamide-induced HCC model

Based on the results obtained from *in vitro* MTT anti-proliferation assay of tested compounds on tumor cell lines, the cytotoxic effects of compounds 5 and 6 were further investigated in HCC model. Male Sprague-Dawley rats were administered 200 mg/kg thioacetamide (TAA) in normal saline, intraperitoneally (i.p.) twice

weekly for 16 weeks to induce HCC [40, 41]. Surviving animals were then randomly allocated into four groups (n = 8/group), which received the following treatments for further two weeks:

• HCC group: received 1% DMSO (500 µL/day, i.p.).

• HCC-C5 and HCC-C6 groups: received compounds 5 and 6, respectively, at a dose of 10 mg/kg/day (diluted in 1% DMSO to a final volume of 500 µL/day, i.p.).

• HCC-DOXO group: received DOXO (1 mg/kg, dissolved in distilled water, i.p, twice weekly).

The study controls included three groups of age-matched normal rats (n = 8/group) that received equal doses of both TAA and compounds vehicle (control group) or both TAA vehicle and the compounds 5/6 (C5 and C6 groups) in a similar manner to those administered to HCC-treated groups. The dose of DOXO administered to HCC rats was previously described [41].

Animal sacrifice and sample collection

At the end of the experiment, blood was collected from anesthetized rats (sodium pentobarbital, 40 mg/kg, i.p.) by retro-orbital puncture using capillary hematocrit tubes. Blood samples were kept at room temperature for 30 minutes and centrifuged (3000×g for 15 minutes) to obtain serum for biochemical analyses. Animals were then sacrificed by cervical dislocation and livers were isolated and washed with ice-cold physiological saline (0.9% NaCl). A small part from right lobe of liver was removed and fixed in 10% neutral buffered formalin for histopathological and immunohistochemical assessments. The remaining liver tissues were kept in liquid nitrogen for subsequent analyses.

Morphometric assessment of in vivo liver tumors

After rat sacrifice, livers of the study groups were morphologically examined for visible tumor nodules in hepatic tissues. Neoplastic nodules of 2 mm diameter or more in each rat liver were counted by two independent investigators who were unaware of the experimental design [5].

Serum biochemical parameters

Commercially available rat ELISA kits were used to assess serum levels of alanine and aspartate transaminase (ALT and AST, respectively; MyBioSource, San Diego, USA), alkaline phosphatase (ALP; BioVision, Milpitas, CA, USA) and α-fetoprotein (Elabscience, Wuhan, China) in accordance with the manufacturer's instructions.

Hepatic levels of transforming growth factor-β1 (TGF-β1), interleukin-1β (IL-1β) and tumor necrosis factor-α (TNF-α)

ELISA kits from MyBioSource, Elabscience and BioLegend (San Diego, USA) were used to determine protein levels of TGF-β1, IL-1β and TNF-α, respectively, in liver tissue homogenates (10% w/v in 0.05 M phosphate buffer, pH 7.4).

Histopathological and immunohistochemical analyses

Formalin-fixed hepatic tissues were embedded in paraffin wax, cut into 4 µm-thick sections and stained with hematoxylin and eosin (H & E) and Masson's trichrome stains. Moreover, additional sections were used for immunohistochemical detection using primary antibodies for α-smooth muscle actin (α-SMA, 1:100, catalog number GTX100034, GeneTex, CA, USA), caspase-3 (1:200, catalog number GTX30246, GeneTex), MyD88 (1:100, catalog number AF5195, Affinity Biosciences, OH. USA) and TRAF-6 (1:100, AF5376, Affinity Biosciences). The percentages areas of fibrosis and positive protein immunostaining in acquired images of liver tissues were assessed using ImageJ Software (National Institutes of Health, USA). All histopathological and immunohistochemical assessments were performed by two independent pathologists who were blinded to experimental grouping.

Western blotting analysis

Proteins were extracted from rat liver tissues using ReadyPrep protein extraction kit (Bio-Rad Laboratories Inc., CA, USA) and Bradford protein assay kit (Bio-Rad) was used to determine protein concentration. Samples were loaded on polyacrylamide gels (20 µg protein/sample), separated by SDS-PAGE and transferred to PVDF membrane. The membranes were blocked in tris-buffered saline with tween 20

Table 1. Cytotoxicity (IC_{50}, μM) of compounds 1-7 and doxorubicin (DOXO) on human cancer cell lines

	Cell lines				
	PC-3	HCT-116	MCF-7	Hela	Hep-G2
Compound 1	39.25 ± 3.2	25.23 ± 2.3	28.39 ± 2.6	23.61 ± 1.9	19.90 ± 1.6
Compound 2	61.90 ± 4.1	41.31 ± 3.3	54.58 ± 4.0	30.63 ± 2.7	35.11 ± 2.9
Compound 3	33.60 ± 2.9	17.69 ± 1.5	16.83 ± 1.4	9.33 ± 1.0	12.94 ± 1.3
Compound 4	46.12 ± 3.4	27.27 ± 2.5	43.34 ± 3.5	17.84 ± 1.6	11.61 ± 1.2
Compound 5	21.35 ± 1.7	9.65 ± 0.9	11.05 ± 1.2	8.18 ± 0.9	7.70 ± 0.6
Compound 6	10.09 ± 1.0	6.25 ± 0.7	8.49 ± 0.9	6.87 ± 0.6	3.86 ± 0.2
Compound 7	29.02 ± 3.1	20.07 ± 2.1	24.37 ± 2.0	13.54 ± 1.4	7.98 ± 0.8
DOXO	8.87 ± 0.6	5.23 ± 0.3	4.17 ± 0.2	5.57 ± 0.4	4.50 ± 0.2

Data are shown as means ± SEM of 3 separate experiments performed in duplicate, DOXO: doxorubicin, PC-3: prostate cancer, HCT-116: colorectal carcinoma, MCF-7: breast cancer, Hela: human cervical epithelioid carcinoma, Hep-G2: hepatocellular carcinoma, IC_{50}: the concentration that inhibits cell growth by 50%.

(TBST) and 3% bovine serum albumin (BSA) and probed with the following primary antibodies from Santa Cruz Biotechnology (CA, USA): TLR4 (1:800, sc-293072), NFκB-p65 (1:800, sc-8008), sEH (1:600, sc-166961). Anti-p NF-κB p65 antibody (Ser536) was purchased from Cell Signaling Technology (Danvers, MA, USA). Subsequently, membranes were incubated with secondary horseradish peroxidase conjugated antibody. The chemiluminescent substrate (Clarity Western ECL substrate, Bio-Rad) was applied to the blots and the chemiluminescent signals were captured using a CCD camera-based imager. The band intensities of target proteins were normalized against the levels of the β-actin housekeeping control (for sEH and TLR4) or against total NF-κB p65 levels (for p NF-κB p65).

Statistical analysis

Data were shown as mean ± SEM. Statistics were carried out using one-way analysis of variance (ANOVA) followed by Tukey's post-hoc test. Statistical analyses and graphing were performed using GraphPad Prism 7 software (CA, USA). Differences were considered significant at $P < 0.05$.

Results

In vitro cytotoxic effects

The *in vitro* cytotoxic effects of the adamantyl isothiourea derivatives 1-7 and the potent anticancer drug Doxorubicin (DOXO) against all assayed human tumor cell lines are depicted in **Table 1**. The results revealed that the compounds showed varying degrees of inhibition of tumor cell proliferation. In general, the cytotoxic effect of the morpholine derivatives 5, 6 and 7 was higher than their 4-phenylpiperazine analogues 1-4, and the best activity was generally attained against the HCC Hep-G2, human cervical epithelioid carcinoma Hela and colorectal carcinoma HCT-116 tumor cell lines. The optimum cytotoxic activity was attained for compounds 5 and 6 which displayed $IC_{50} < 10$ μM against three and four cell lines, respectively. Based on these results, compounds 5 and 6 are considered as good candidates for further investigation as potential chemotherapeutic agents for HCC and their *in vivo* cytotoxic activity in TAA-induced HCC rat model was studied.

Serum biochemical parameters in TAA-administered rats

HCC rats showed significant elevations in serum levels of ALT, AST, ALP and α-fetoprotein as compared to control group ($P < 0.0001$ for all, **Figure 3A-D**). Compounds 5 and 6 significantly reduced serum activities of ALT, AST and ALP in HCC rats ($P < 0.0001$ vs. HCC group) to levels that were insignificantly different to those observed in HCC-DOXO group ($P > 0.05$). Compared to untreated HCC group, compounds 5 and 6 significantly diminished serum α-fetoprotein levels by 35.2% ($P < 0.0001$ vs. both HCC and HCC-DOXO groups) and 43.9% ($P < 0.0001$ vs. HCC group, $P > 0.05$ vs. HCC-DOXO group), respectively.

In vivo liver tumors in TAA-administered rats

As shown in **Figure 4**, livers from control, C5 and C6 groups showed normal glossy-brown appearance with soft smooth texture. Conversely, HCC rat livers were bigger in size with a

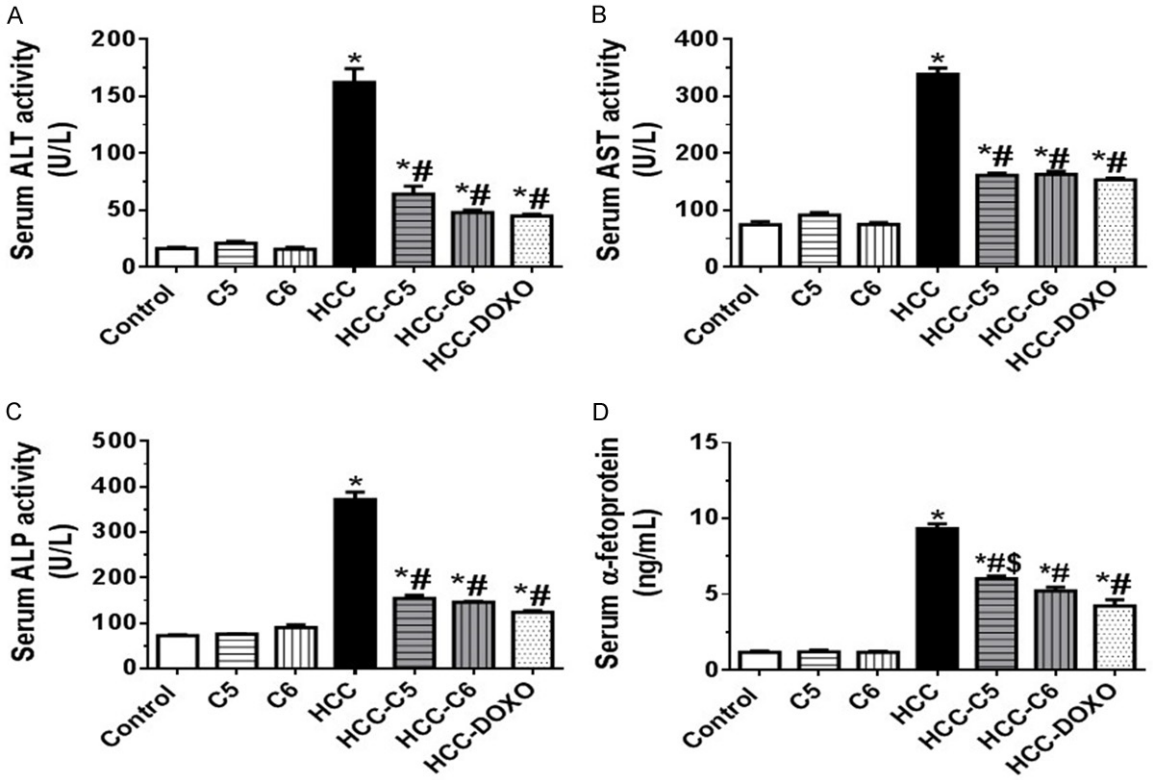

Figure 3. Effect of compounds 5 and 6 on serum levels of ALT (A), AST (B), ALP (C) and α-fetoprotein (D) in TAA-administered rats. Data are presented as mean ± SEM, n = 8/group. $^{*}P < 0.05$ vs. control group, $^{\#}P < 0.05$ vs. HCC group, $^{\$}P < 0.05$ vs. HCC-DOXO group. ALT: alanine transaminase, ALP: alkaline phosphatase, AST: aspartate transaminase, DOXO: doxorubicin, HCC: hepatocellular carcinoma, TAA: thioacetamide.

rough granulose cirrhotic appearance compared to those of control groups. Moreover, white to reddish nodules were consistently visible on the surface of livers from all untreated HCC rats (percentage incidence = 8/8; 100%). On the other hand, HCC rats treated with compounds 5, 6 and DOXO showed improved liver morphology and reduced cirrhotic changes as compared to untreated HCC group. Additionally, the numbers of visible hepatic nodules in HCC-C5 (percentage incidence = 7/8; 87.5%), HCC-C6 (percentage incidence = 5/8; 62.5%) and HCC-DOXO (percentage incidence = 5/8; 62.5%) groups were significantly lower than those of untreated HCC rats. Interestingly, C6 treatment reduced number of liver nodules in HCC rats to a level that was not significantly different from numbers brought about by DOXO treatment.

Hepatic histopathological alterations in TAA-administered rats

H&E-stained hepatic tissues from the study groups are shown in **Figure 5**. Liver specimens from control, C5 and C6 groups exhibited normal arrangement of hepatic cords around the central veins with normal portal areas and sinusoids.

In contrast, liver tissues from HCC group demonstrated well-differentiated HCC tumor cells that were separated from the non-tumorous hepatic tissue by a vascularized capsule. HCC tumor cells were polygonal with eosinophilic granular cytoplasm, rounded vesicular nuclei with coarse chromatin, higher nuclear-cytoplasmic ratio, multiple nuclei and cytoplasmic and nuclear eosinophilic inclusions. Moreover, non-tumorous hepatic tissues in HCC rats showed loss of normal hepatic architecture due to arrangement of hepatocytes in solid nodules without central vein and subdivided by thick fibrous septa. These nodules also demonstrated leukocytes infiltration, proliferated bile ductules and congested blood vessels. Some other nodules showed hydropic to ballooning degeneration with ground-glass hepatocytes characterized by vacuolated cytoplasm with apoptotic nuclei and micro to macro-vesicular steatosis.

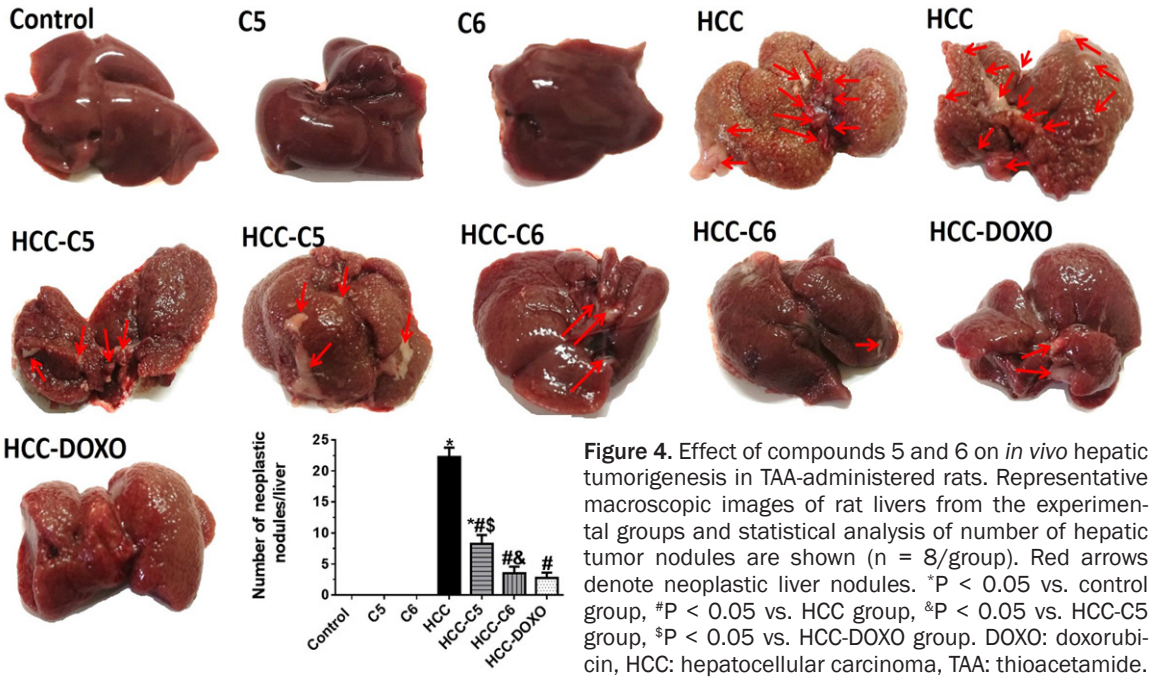

Figure 4. Effect of compounds 5 and 6 on *in vivo* hepatic tumorigenesis in TAA-administered rats. Representative macroscopic images of rat livers from the experimental groups and statistical analysis of number of hepatic tumor nodules are shown (n = 8/group). Red arrows denote neoplastic liver nodules. $^{*}P < 0.05$ vs. control group, $^{\#}P < 0.05$ vs. HCC group, $^{\&}P < 0.05$ vs. HCC-C5 group, $^{\$}P < 0.05$ vs. HCC-DOXO group. DOXO: doxorubicin, HCC: hepatocellular carcinoma, TAA: thioacetamide.

The hepatocytes on the periphery of the nodules were necrotic.

These pathological changes in liver tissues were markedly reduced in HCC rats treated with compounds 5, 6 and DOXO, leading to partially retained normal organization of hepatic tissues, which only showed thin fibrous strands extending from portal areas, periportal macrovesicular steatosis with few necrotic cells and mild congestion. Liver sections from HCC-C6 group had slightly less pronounced lesions than those from HCC-C5 rats.

Hepatic cirrhosis in TAA-administered rats

Masson's trichrome-stained hepatic sections (**Figure 6**) showed no fibrosis in control, C5 and C6 groups. In contrast, liver tissues from HCC rats demonstrated disrupted parenchymal structure due to extensive deposition of dense blue stained fibrous tissue containing dilated blood vessels, dividing hepatic parenchyma into solid nodules lacking normal structures of hepatic lobules. On the other hand, hepatic sections from HCC-C5 group exhibited moderate light blue stained fibrous tissue deposition in portal areas. Similarly, the HCC rats treated with compound 6 showed mild to moderate light blue stained fibrous tissue deposition in hepatic portal areas. Liver tissues from HCC-DOXO rats demonstrated thin strands of light blue stained fibrous tissue deposition in portal areas. Statistical analysis of percentages of collagen deposition areas in hepatic sections from the study groups showed a significant reduction in fibrosis percentage in HCC-C5, HCC-C6 and HCC-DOXO groups when compared with untreated HCC group ($P < 0.0001$ for all groups).

Hepatic α-SMA expression

Whereas liver tissues from control, C5 and C6 groups showed negative α-SMA immunoexpression, hepatic sections from HCC group demonstrated marked immunopositivity against α-SMA mainly around hepatic solid nodules. Hepatic tissues from HCC-C5 group showed moderate positive α-SMA immunostaining in portal areas, while those from HCC-C6 rats exhibited mild to moderate positive α-SMA immunoexpression against α-SMA in portal areas. The hepatic sections from HCC-DOXO group showed weak positive expression against α-SMA in portal areas (**Figure 7**).

Statistical analysis of percentages of α-SMA-immunostained areas showed a significant reduction in α-SMA immunoexpression in HCC-C5, HCC-C6 and HCC-DOXO groups when compared with untreated HCC group ($P < 0.0001$ for all groups).

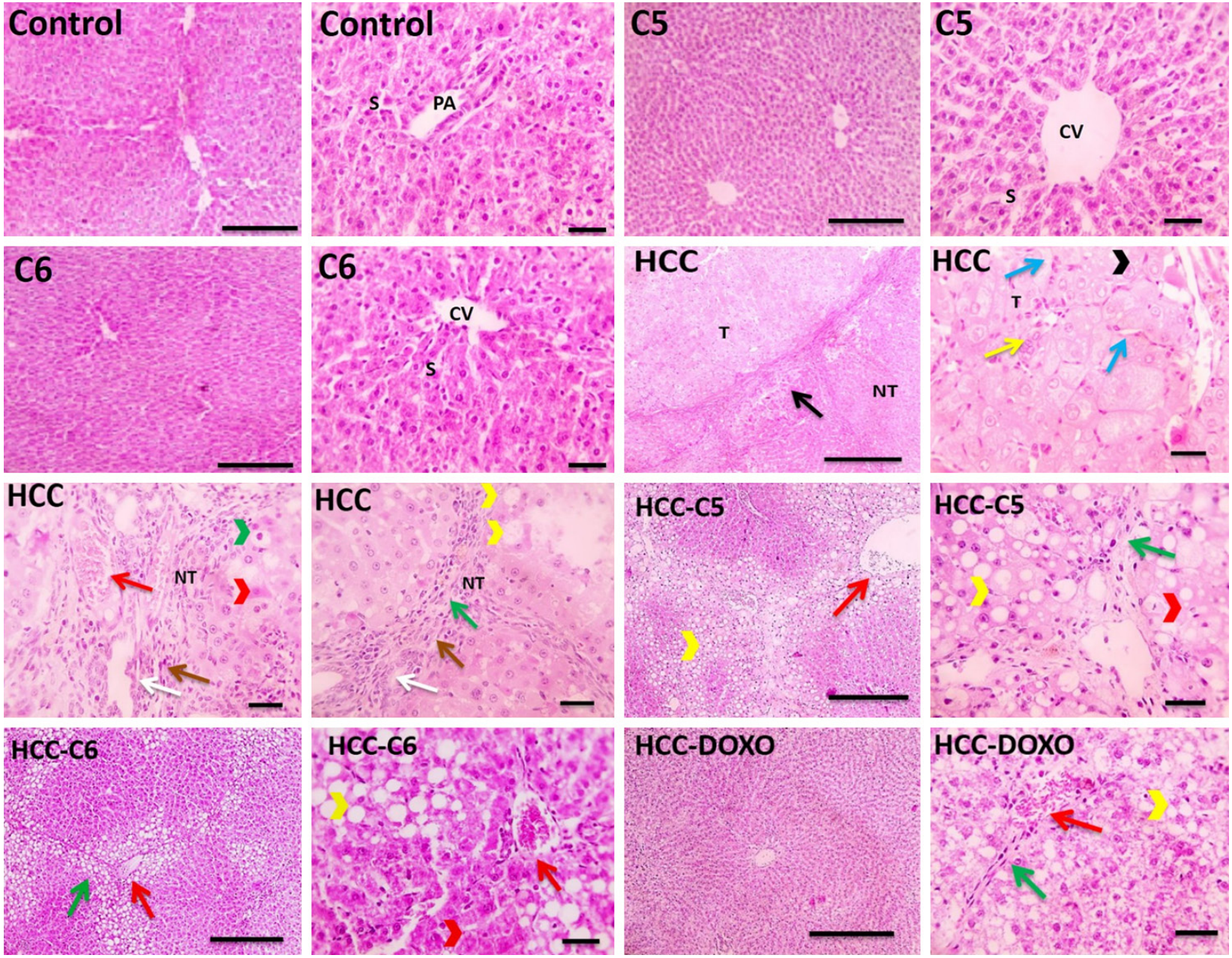
Control
Control
S
PA
C5
C5
CV
S
C6
C6
CV
S
HCC
T
NT
HCC
T
HCC
NT
HCC
NT
HCC-C5
HCC-C5
HCC-C6
HCC-C6
HCC-DOXO
HCC-DOXO

Figure 5. Representative microimages of H & E-stained hepatic tissues from the experimental groups. Images were captured at magnification of 100× (scale bar, 100 μm) or 400× (scale bar, 50 μm). The arrow color represents; black: vascularized capsule, brown: infiltrated leukocytes, blue: hypertrophied nuclei of Kupffer cells, green: fibrous septa, red: congested blood vessels, white: proliferated bile ductules, yellow: multiple nuclei. The arrowhead color represents; black: eosinophilic inclusions, green: apoptotic nuclei, red: necrotic hepatocytes, yellow: vesicular steatosis. CV: central vein. DOXO: doxorubicin, HCC: hepatocellular carcinoma, H & E: hematoxylin and eosin, NT: non-tumor cells, PA: portal areas, S: sinusoids, T: tumor cells.

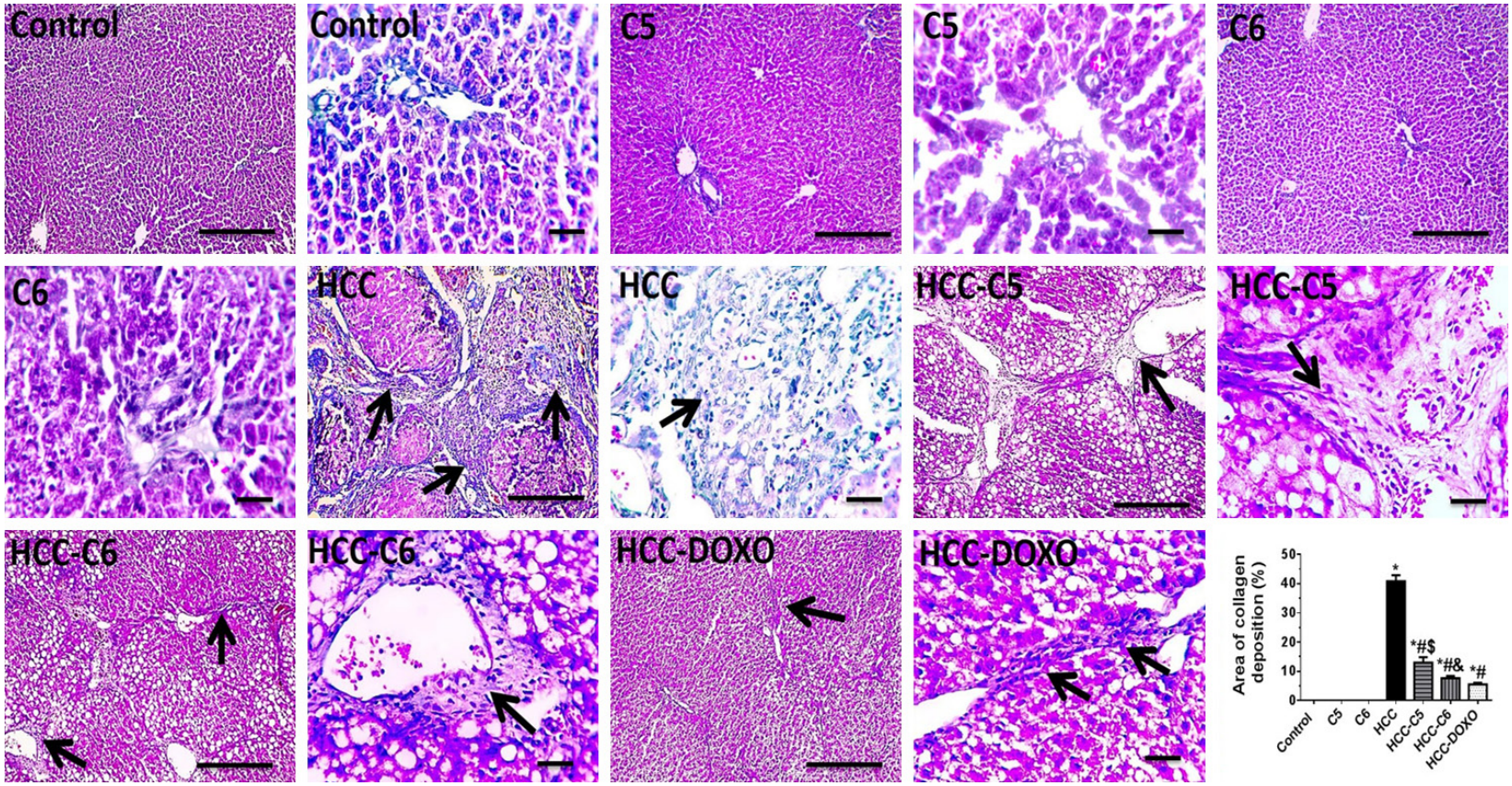

Figure 6. Representative microimages of Masson's trichrome-stained hepatic tissues from the experimental groups. Images were captured at magnification of 100× (scale bar, 100 μm) or 400× (scale bar, 50 μm). Black arrows point to areas of fibrosis. Statistical analysis of area of collagen deposition in hepatic sections is shown. $^{*}P < 0.05$ vs. control group, $^{\#}P < 0.05$ vs. HCC group, $^{\&}P < 0.05$ vs. HCC-C5 group, $^{\$}P < 0.05$ vs. HCC-DOXO group. DOXO: doxorubicin, HCC: hepatocellular carcinoma.

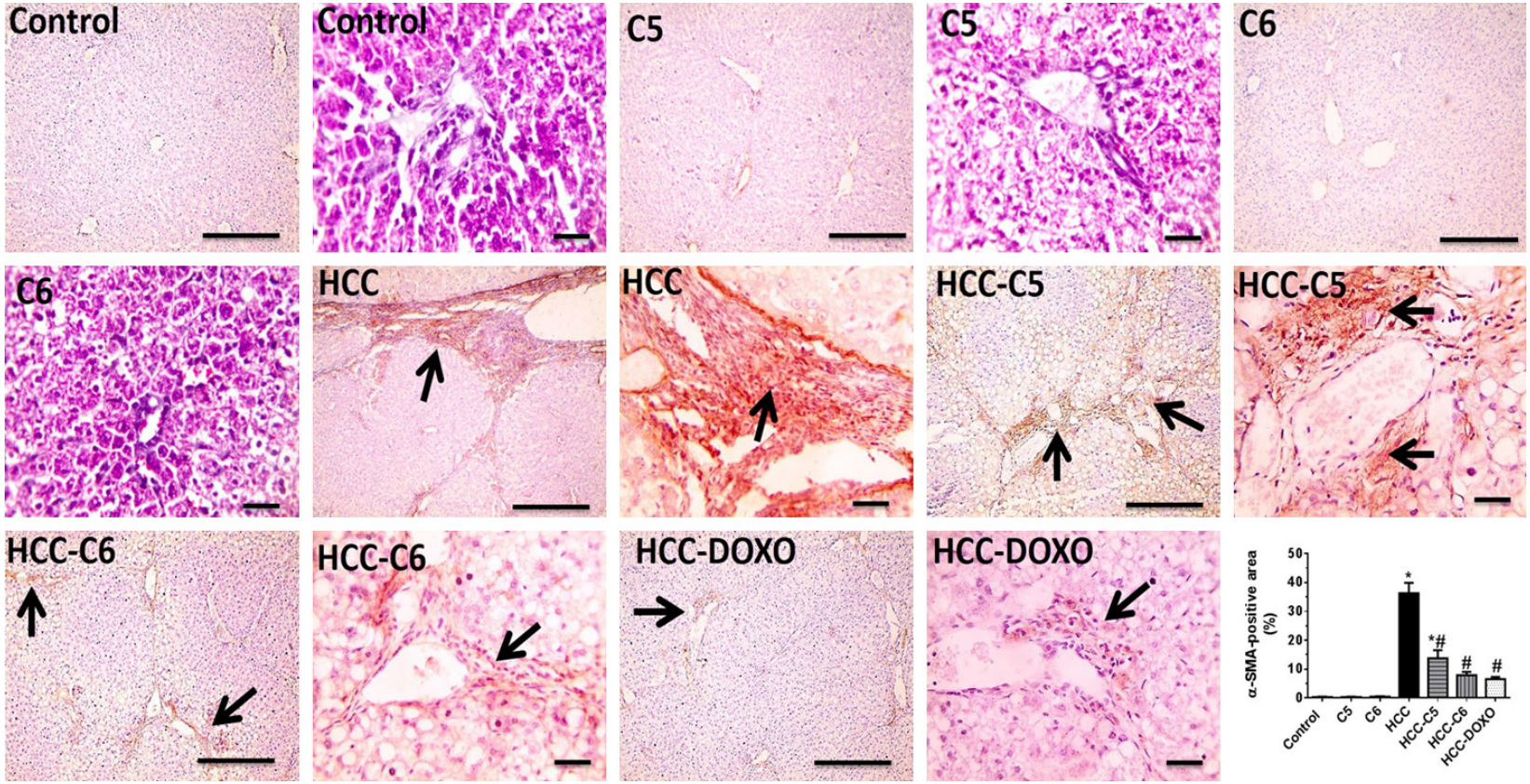

Figure 7. Effect of compounds 5 and 6 on hepatic α-SMA protein expression in TAA-administered rats. Representative microimages of immunostaining for α-SMA protein (IHC counterstained with Mayer's hematoxylin) in hepatic tissues and statistical analysis of positive area of immunolabelling (%) are shown. Black arrows denote positive immunoexpression. Images were captured at magnification of 100× (scale bar, 100 μm) or 400× (scale bar, 50 μm). $^{*}P < 0.05$ vs. control group, $^{\#}P < 0.05$ vs. HCC group. α-SMA: α-smooth muscle actin. DOXO: doxorubicin, HCC: hepatocellular carcinoma, IHC: immunohistochemistry, TAA: thioacetamide.

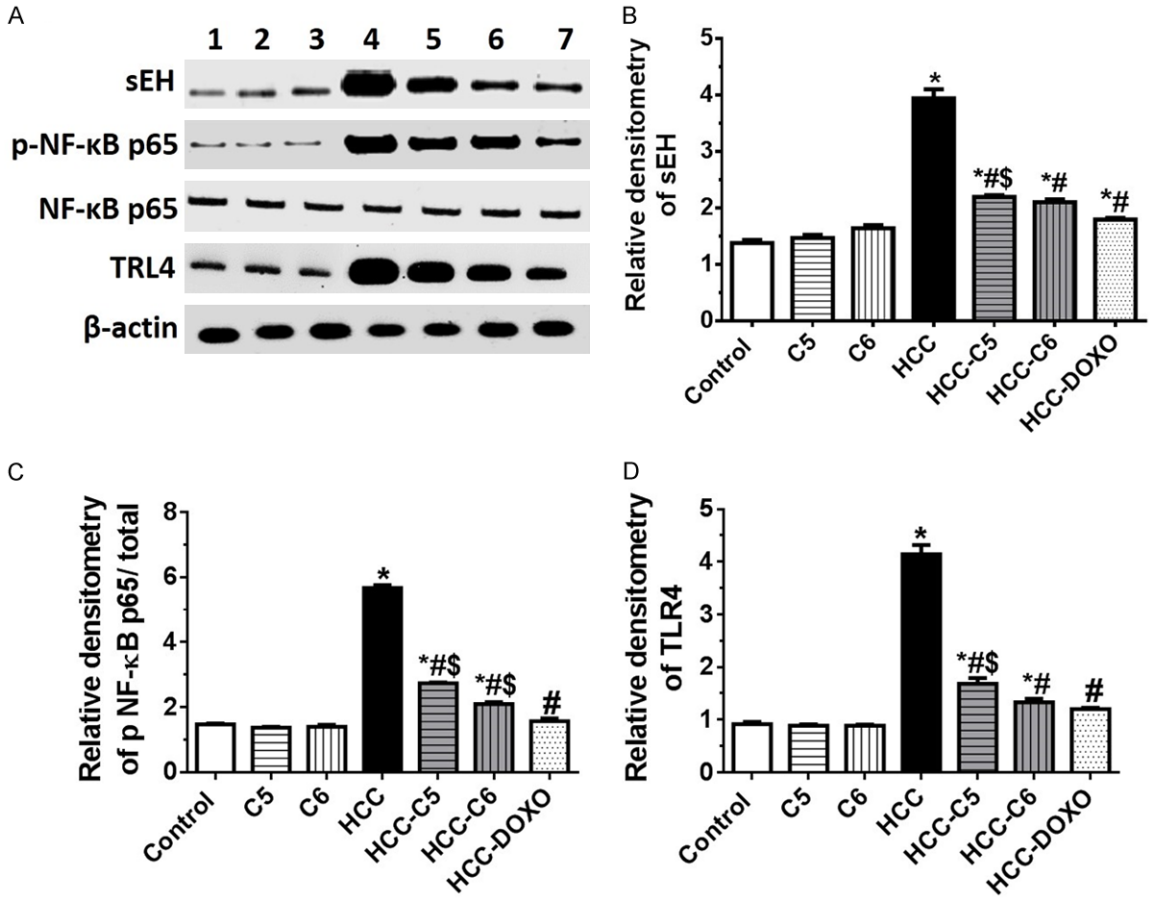

Figure 8. Effect of compounds 5 and 6 on hepatic expression of sEH, p-NF-κB p65 and TLR4 in TAA-administered rats. A: Western blot detection of hepatic expression levels of sEH, p NF-κB p65, total NF-κB p65 and TLR4. (1) Control group, (2) C5 group, (3) C6 group, (4) HCC group, (5) HCC-C5 group, (6) HCC-C6 group, (7) HCC-DOXO group. The blots were cropped and whole full-length blots are shown in Figure S1. B-D: Quantitative analyses of relative expression of sEH, p NF-κB p65/total and TLR4, respectively. Data are presented as mean ± SEM of 3-4 independent experiments. $^{*}P < 0.05$ *vs.* control group, $^{\#}P < 0.05$ vs. HCC group, $^{\$}P < 0.05$ vs. HCC-DOXO group. DOXO: doxorubicin, HCC: hepatocellular carcinoma, p-NF-κB p65: phosphorylated nuclear factor-κB p65, sEH: soluble epoxide hydrolase, TAA: thioacetamide, TLR4: toll-like receptor 4.

Hepatic expression of sEH, p-NF-κB p65 and TLR4

In HCC rats, the hepatic levels of sEH, p-NF-κB p65 and TLR4 were significantly increased as compared with levels in control group (**Figure 8A-D**). Moreover, Western blot analysis revealed that liver tissues from HCC-C5, HCC-C6 and HCC-DOXO exhibited significantly lower expression levels of sEH, p-NF-κB p65 and TLR4 proteins compared to those of untreated HCC group ($P < 0.0001$ for all comparisons).

Hepatic MyD88 and TRAF-6 expression

Figures 9 and **10** show immunohistochemical labeling of MyD88 and TRAF-6 proteins, respectively, in hepatic tissues. Negative MyD88 and TRAF-6 immunostaining of hepatocytes was observed in control, C5 and C6 groups. In contrast, hepatic sections from HCC group exhibited marked increase of positive immunostaining against MyD88 (**Figure 9**) and TRAF-6 (**Figure 10**). On the other hand, hepatic sections from HCC-C5 group showed multifocal positive immunolabeling areas against MyD88, while HCC rats treated with compound 6 demonstrated few focal positive immunostained areas of MyD88 (**Figure 9**). Similarly, mild positive immunolabeling against TRAF-6 was noticed in HCC-C5 and HCC-C6 tissues (**Figure 10**). Hepatic tissues from HCC-DOXO group showed marked decreases in positive immunoreactivity against both MyD88 and TRAF-6.

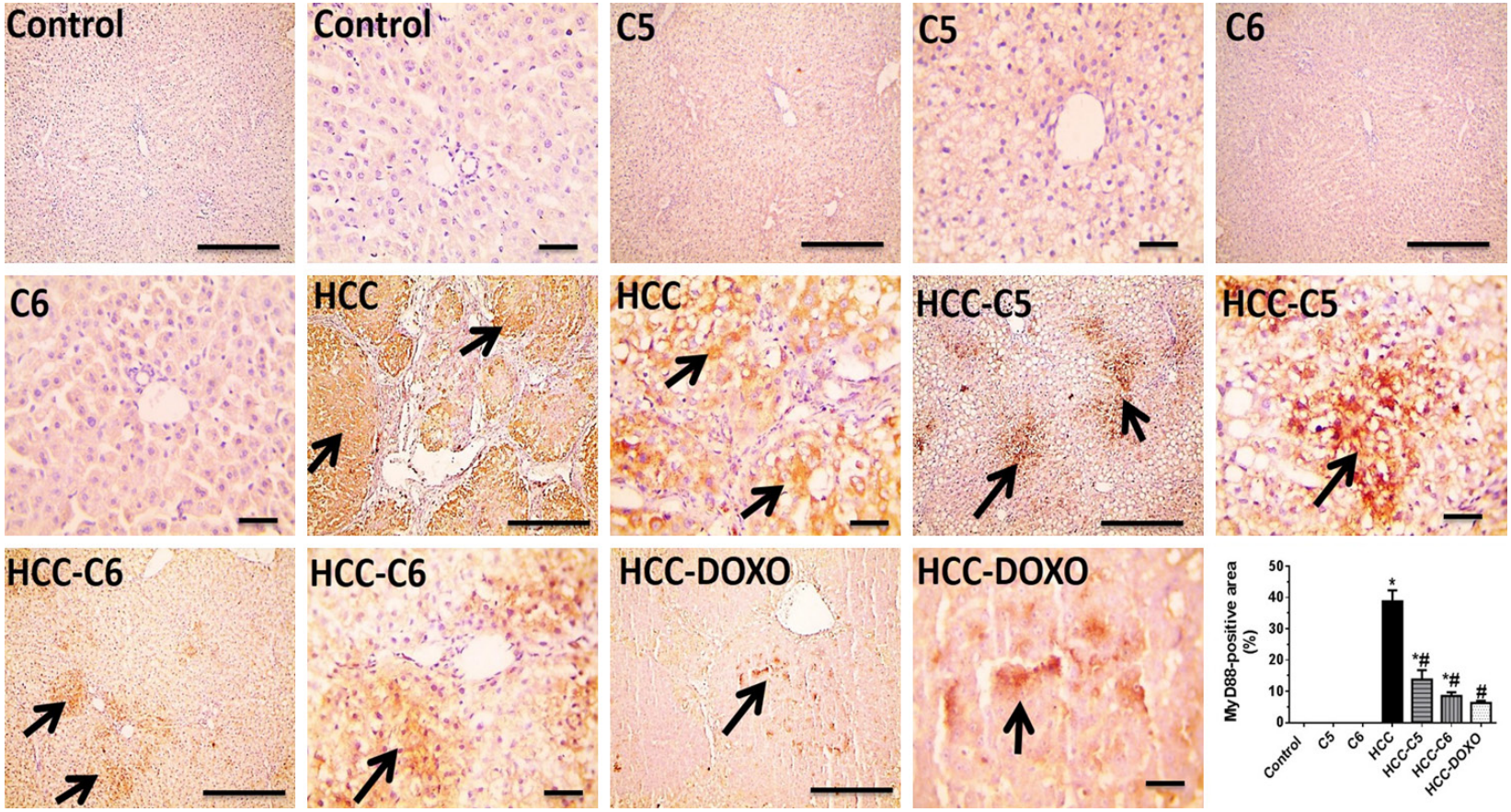

Figure 9. Effect of compounds 5 and 6 on hepatic MyD88 protein expression in TAA-administered rats. Representative microimages of immunostaining for MyD88 protein (IHC counterstained with Mayer's hematoxylin) in hepatic tissues and statistical analysis of positive area of immunolabelling (%) are shown. Black arrows denote positive immunoexpression. Images were captured at magnification of 100× (scale bar, 100 μm) or 400× (scale bar, 50 μm). $^{*}P < 0.05$ vs. control group, $^{\#}P < 0.05$ vs. HCC group. DOXO: doxorubicin, HCC: hepatocellular carcinoma, IHC: immunohistochemistry, MyD88: myeloid differentiation primary response-88, TAA: thioacetamide.

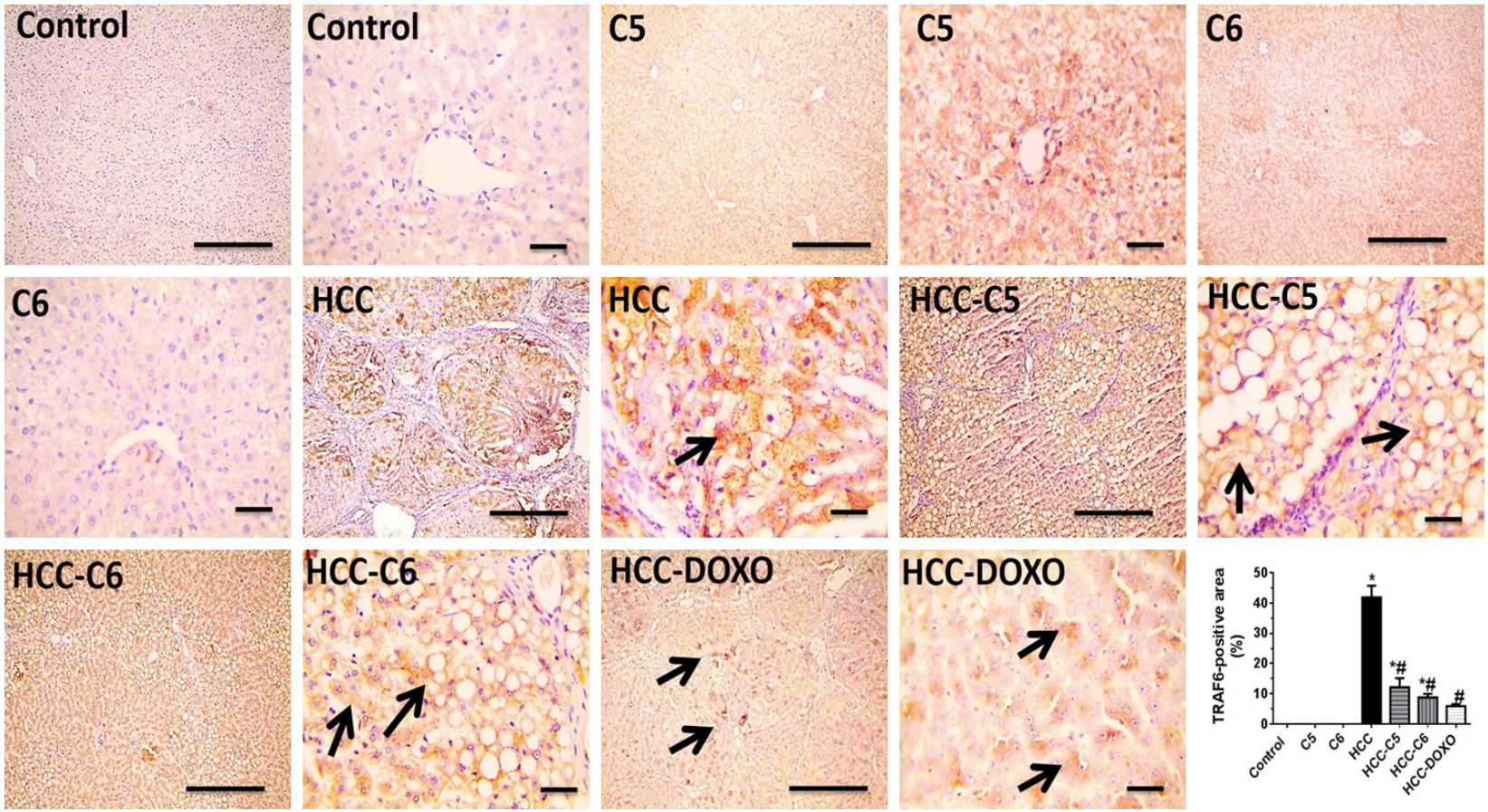

Figure 10. Effect of compounds 5 and 6 on hepatic on hepatic TRAF-6 protein expression in TAA-administered rats. Representative microimages of immunostaining for TRAF-6 protein (IHC counterstained with Mayer's hematoxylin) in hepatic tissues and statistical analysis of positive area of immunolabelling (%) are shown. Black arrows denote positive immunoexpression. Images were captured at magnification of 100× (scale bar, 100 μm) or 400× (scale bar, 50 μm). $^{*}P < 0.05$ vs. control group, $^{\#}P < 0.05$ vs. HCC group. DOXO: doxorubicin, HCC: hepatocellular carcinoma, IHC: immunohistochemistry, TAA: thioacetamide, TRAF-6: tumor necrosis factor receptor-associated factor-6.

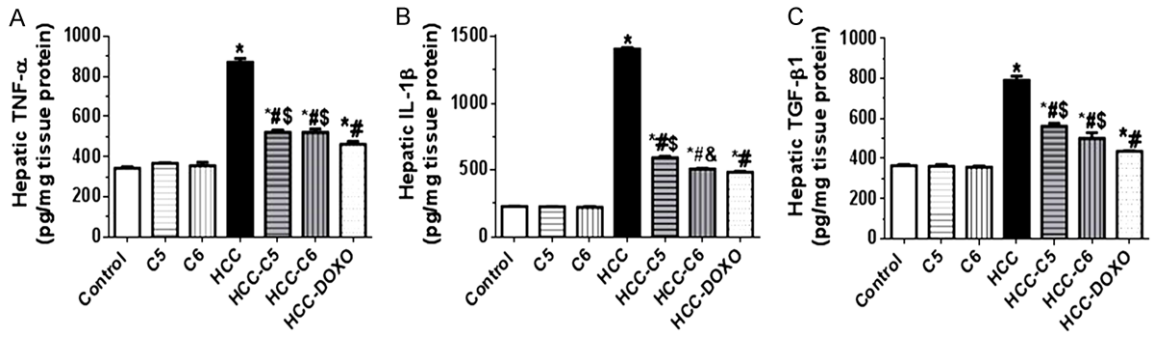

Figure 11. Effect of compounds 5 and 6 on hepatic levels of TNF-α (A), IL-1β (B) and TGF-β1 (C) in TAA-administered rats. Data are presented as mean ± SEM, n = 8/group. $^{*}P < 0.05$ vs. control group, $^{\#}P < 0.05$ vs. HCC group, $^{\&}P < 0.05$ vs. HCC-C5 group, $^{\$}P < 0.05$ vs. HCC-DOXO group. DOXO: doxorubicin, HCC: hepatocellular carcinoma, IL-1β: interleukin-1β, TAA: thioacetamide, TGF-β1: transforming growth factor-β1, TNF-α: tumor necrosis factor- α.

Statistical analyses of positive areas of immunolabeling (%) against MyD88 and TRAF-6 in immunostained hepatic sections showed significant increases of immunolabeling areas in HCC group compared to control group ($P < 0.0001$), which was significantly reduced in HCC-C5, HCC-C6 and HCC-DOXO groups compared to untreated HCC group.

Hepatic levels of TNF-α, IL-1β and TGF-β1

HCC liver tissues showed significant increases in levels of TNF-α (by 2.5-fold, **Figure 11A**), IL-1β (by 6.2-fold, **Figure 11B**) and TGF-β1 (by 2.2-fold, **Figure 11C**) compared to control levels ($P < 0.0001$ vs. control group for all cytokine levels).

Treatment of HCC rats with compounds 5 and 6 significantly reduced hepatic levels of TNF-α (by 40.0% and 40.1%, respectively), IL-1β (by 58.0% and 63.9%, respectively) and TGF-β1 (by 29.1% and 36.5%, respectively) compared to untreated HCC group. The attenuative effects of compound 6 on hepatic cytokine levels were comparable to, but still significantly different from, those observed in HCC-DOXO rats, which showed decreases in TNF-α, IL-1β and TGF-β1 levels by 47.0%, 65.7% and 45.0%, respectively, relative to HCC group.

Hepatic caspase-3 expression

Liver tissues from control, C5 and C6 groups showed mild positive caspase-3 immunostaining of hepatocytes cytoplasm. Conversely, hepatic sections from HCC group exhibited a marked decrease of positive immunolabelling against caspase-3. On the other hand, hepatic tissues from HCC-C5 rats showed mild positive immunolabelling against caspase-3 in few hepatocytes, while hepatic sections from HCC-C6 group demonstrated multifocal positive immunoreactive areas against caspase-3. The hepatic specimens from HCC-DOXO group showed marked increase in caspase-3 immunoexpression (**Figure 12**).

Statistical analysis of percentages of caspase-3-immunostained areas showed a significant increase in caspase-3 immunoexpression in HCC-C5 ($P < 0.05$), HCC-C6 ($P < 0.001$) and HCC-DOXO ($P < 0.0001$) groups when compared with untreated HCC group.

Discussion

HCC is one of the most life-threatening cancer types, accounting for 8.2% of cancer-related death worldwide [1]. Current chemotherapy of HCC is generally ineffective, and thus novel treatments that diminish mortality and increase survival rates are warranted [42]. In the present study, *in vitro* cytotoxic activity of the adamantyl isothiourea derivatives 1-7 was assessed against five human tumor cell lines. The compounds displayed marked cytotoxic effect and the optimum activity was attained for compounds 5 and 6 (IC_{50} values were 7.70 and 3.86 μM, respectively) particularly against the HCC Hep-G2 tumor cell lines. Accordingly, compounds 5 and 6 could be considered as promising candidates for further investigation as potential chemotherapeutic agents for HCC and their *in vivo* cytotoxic activity in TAA-induced HCC rat model was thus evaluated.

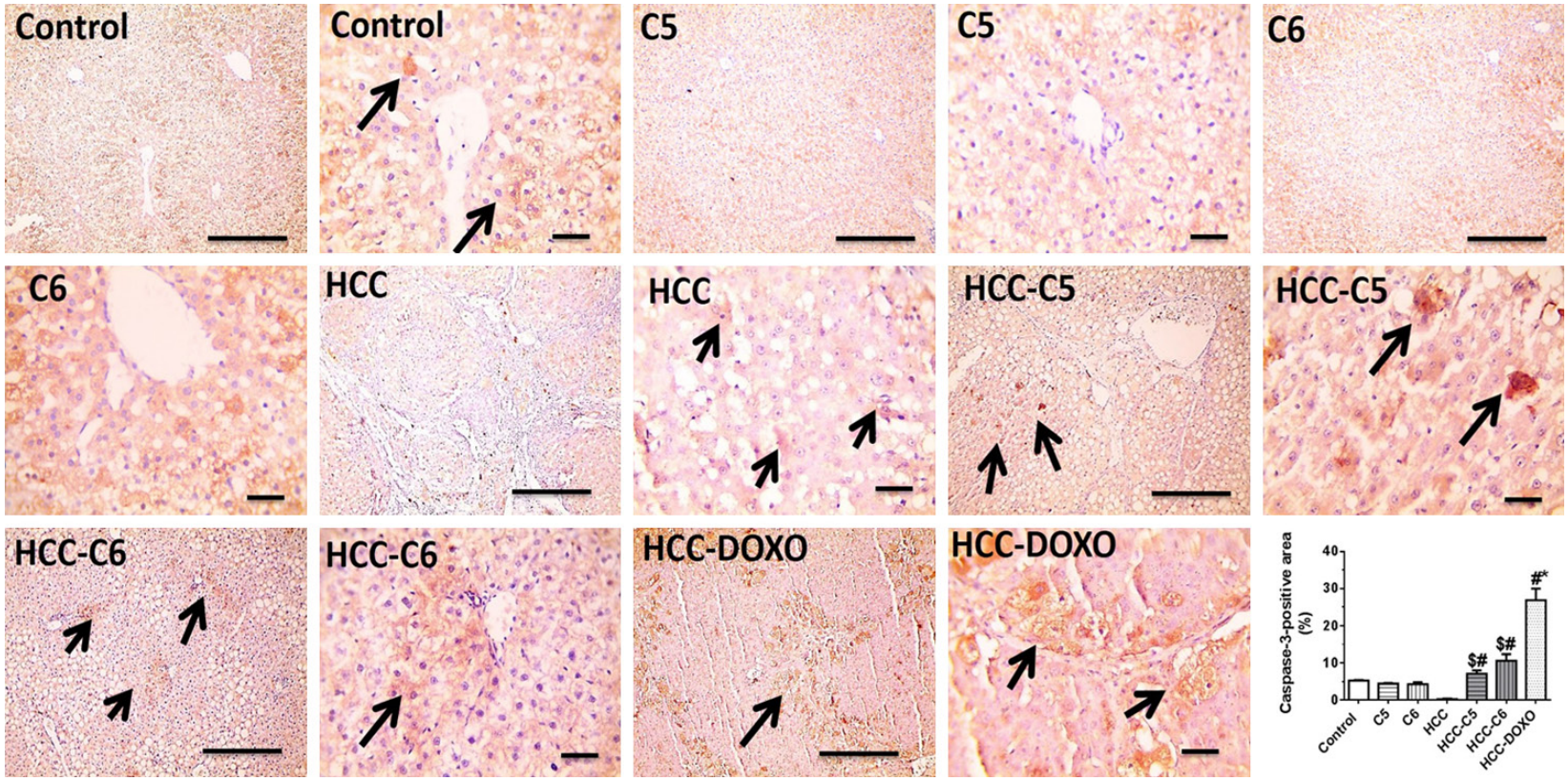

Figure 12. Effect of compounds 5 and 6 on hepatic caspase-3 protein expression in TAA-administered rats. Representative microimages of immunostaining for caspase-3 protein (IHC counterstained with Mayer's hematoxylin) in hepatic tissues and statistical analysis of positive area of immunolabelling (%) are shown. Black arrows denote positive immunoexpression. Images were captured at magnification of 100× (scale bar, 100 μm) or 400× (scale bar, 50 μm). $^{*}P < 0.05$ vs. control group, $^{\#}P < 0.05$ vs. HCC group, $^{\$}P < 0.05$ vs. HCC-DOXO group. DOXO: doxorubicin, HCC: hepatocellular carcinoma, IHC: immunohistochemistry, TAA: thioacetamide.

Moreover, in TAA-induced HCC rat model, compounds 5 and 6 elicited the following beneficial effects: a) they significantly reduced serum levels of ALT, AST and ALP and α-fetoprotein, b) they suppressed hepatocarcinogenesis and diminished liver fibrosis, inflammation and other histopathological alterations, c) they reduced hepatic protein expression levels of α-SMA, sEH, p-NF-κB p65, TLR4, MyD88, TRAF-6, TNF-α, IL-1β and TGF-β1 and d) they increased caspase-3 expression in liver tissues of HCC rats. In most assessments, the effects of compound 6 were more comparable, than were those of compound 5 to the cytotoxic effects of DOXO.

Chronic TAA administration was used to induce HCC in rats. This model involves chronic liver damage, inflammation, fibrogenesis, cirrhosis, neoplastic nodules and enhanced levels of the TLR4 ligand LPS, and therefore shares multiple aspects with human HCC tumor microenvironment [7, 40, 43, 44]. DOXO is an established antineoplastic agent which is extensively used for chemotherapy of solid cancers, including HCC [45-48].

The development of HCC tumors in TAA-administered rats was evidenced by significantly elevated serum levels of α-fetoprotein in HCC group (**Figure 3D**), observed macroscopic hepatic neoplastic nodules (**Figure 4**) and appearance of well-differentiated HCC tumor cells in H & E-stained liver tissues from HCC rats (**Figure 5**). α-Fetoprotein is a robust marker of HCC since its expression is consistently elevated during cirrhosis-associated hepatocarcinogenesis [49]. Serum α-fetoprotein levels were significantly reduced in HCC rats treated with compounds 5 and 6, suggesting that they suppressed HCC tumor growth.

Elevated serum levels of ALT, AST and ALP in HCC rats (**Figure 3A-C**) are potentially attributed to leakage of these enzymes from neoplastic cells or necrotic hepatocytes into circulation [50]. Compounds 5 and 6 significantly diminished serum liver enzyme levels in HCC rats, implying hepatoprotective and/or antitumor effects of these compounds. These findings are supported by histopathological analyses which showed that compounds 5 and 6 partially restored normal organization of hepatic tissues and reduced liver parenchymal damage and hepatocyte necrosis (**Figure 5**). Moreover, they markedly attenuated fibrous tissue deposition in portal areas and improved the hepatic structure (**Figure 6**).

In this work, western blot analyses demonstrated that HCC liver tissues showed elevated expression of sEH relative to controls. Consistently, carbon tetrachloride cirrhotic rats showed upregulated hepatic expression of sEH [30]. Mammalian sEH is a hydrolytic enzyme that degrades epoxy-fatty acids, which possess beneficial anti-inflammatory effects, into less active diols [51, 52]. Therefore, inhibition of sEH is potentially associated with attenuation of inflammation [29]. Interestingly, previous research has shown that adamantyl thiourea derivatives can exhibit inhibitory activity against sEH [26]. In line with this, compounds 5 and 6 reduced hepatic sEH expression in HCC rats, which might contribute to their anti-inflammatory, antifibrotic and anticancer activities. Supporting this notion, sEH inhibition caused suppression of inflammatory TLR4/MyD88/NF-κB signaling pathway in CNS of mice with experimental encephalomyelitis [53]. Moreover, pharmacological inhibition of sEH reduced liver fibrosis in carbon tetrachloride-treated rats [30]. Furthermore, a combination of sEH inhibitor and cyclooxygenase-2 inhibitor suppressed primary lung tumor in mice [31]. Intriguingly, the anticancer agent sorafenib, currently used for treatment of advanced HCC, was reported to inhibit human sEH along with its tyrosine kinase inhibitory effect [54].

Chronic hepatic inflammation is an established risk factor mediating development of fibrosis/cirrhosis and their progression into HCC [55]. TLR4-MyD88-NF-κB signaling cascade was reported to be actively involved in hepatic inflammation-fibrosis-HCC axis [56]. Bacteria from the intestine may cross the intestinal barrier into the portal vein and from there to the liver. Thereafter, engagement of hepatic TLR4 receptors with bacterial products from intestinal microbiota may lead to an inflammatory response that contributes to subsequent long-term liver tissue alterations into HCC [4, 57].

In the present study, HCC liver tissues showed enhanced expression of TLR4, MyD88, TRAF-6 and p-NF-κB p65. This agrees with previous studies on experimental and human HCC tissues [5, 58-60]. The adamantane derivatives 5 and 6 suppressed the hepatic expression levels of these proteins, which might explain their antifibrotic and antitumor effects. Pharma-

cological inhibition of TLR4-MyD88-NF-κB signaling was shown to suppress HCC progression [5, 58]. TLR4-deficient mice showed less fibrosis in experimental fibrosis models, indicating a role of TLR4 in hepatic fibrogenesis [7]. Moreover, mice deficient in TLR4 and MyD88 [11] and mice carrying TLR4-inactive mutant [4] exhibited reduced incidence, number and size of DEN-induced HCC tumors compared to wild type mice. Furthermore, knock-down of TRAF-6 in HCC cell lines resulted in a decrease in their viabilities [60].

Activation of TLR4/MyD88/NF-κB cascade leads to subsequent production of pro-inflammatory cytokines, including IL-1β and TNF-α [61, 62]. It is well established that enhanced hepatic levels of inflammatory cytokines mediate liver inflammation and tumorigenesis [63-65]. In the present study, compounds 5 and 6 significantly reduced hepatic levels of TNF-α and IL-1β in HCC rats, indicating their anti-inflammatory effects that might explain, at least in part, tumor suppression in HCC-C5 and HCC-C6 groups.

Moreover, compounds 5 and 6 significantly reduced hepatic levels of TGF-β1 and attenuated α-SMA expression in liver tissues of HCC rats, which might contribute to their antifibrotic effects. It was reported that TLR4-MyD88-NF-κB axis activates TGF-β signaling, which enhances fibrotic changes in inflamed liver [7] via activating differentiation of hepatic stellate cells and portal fibroblasts into myofibroblasts, increasing α-SMA expression and boosting excessive deposition of extracellular matrix proteins [66]. TGF-β signaling also enhances HCC tumor growth and progression [67].

Declined expression of caspase-3 correlated with poor prognosis in HCC patients, suggesting that it might be implicated in HCC progression. Moreover, caspase-3-deficient mice exhibited a significant increase in DEN-induced HCC [68]. In this work, marked increases in caspase-3 immunoexpression were observed in liver tissues from HCC-C5, HCC-C6 and HCC-DOXO groups when compared with those from untreated HCC rats, suggesting that their antitumor activities against HCC could be attributed to induction of apoptosis of transformed hepatocytes. Previously, DOXO has been shown to significantly increase hepatic caspase-3 mRNA expression in HCC tissues from TAA-administered rats [41]. These effects could be attributed to inhibition of NF-κB activation and inflammatory cytokine production, which mutually enhance tumors survival via suppressing apoptosis of transformed hepatocytes [62].

In conclusion, this research demonstrated that the adamantly isothiourea derivatives 5 and 6 exhibited *in vitro* cytotoxic effects against HCC Hep-G2 cell line and suppressed liver tissue inflammation, fibrosis and tumorigenesis, possibly via reducing expression of sEH and impairing TLR4-MyD88-NF-κB signaling. More investigations are needed to confirm these findings in other experimental HCC models and explore detailed molecular mechanisms that may underlie their antitumor effects.

Acknowledgements

This research was funded by the Deanship of Scientific Research at Princess Nourah bint Abdulrahman University through the Fast-track Research Funding Program.

Disclosure of conflict of interest

None.

Address correspondence to: Ali A El-Emam, Department of Medicinal Chemistry, Faculty of Pharmacy, Mansoura University, Mansoura 35516, Egypt. E-mail: elemam@mans.edu.eg

References

[1] Bray F, Ferlay J, Soerjomataram I, Siegel RL, Torre LA and Jemal A. Global cancer statistics 2018: GLOBOCAN estimates of incidence and mortality worldwide for 36 cancers in 185 countries. CA Cancer J Clin 2018; 68: 394-424.

[2] Forner A, Reig M and Bruix J. Hepatocellular carcinoma. Lancet 2018; 391: 1301-1314.

[3] Moeini A, Cornella H and Villanueva A. Emerging signaling pathways in hepatocellular carcinoma. Liver Cancer 2013; 1: 83-93.

[4] Dapito DH, Mencin A, Gwak GY, Pradere JP, Jang MK, Mederacke I, Caviglia JM, Khiabanian H, Adeyemi A, Bataller R, Lefkowitch JH, Bower M, Friedman R, Sartor RB, Rabadan R and Schwabe RF. Promotion of hepatocellular carcinoma by the intestinal microbiota and TLR4. Cancer Cell 2012; 21: 504-516.

[5] Ding YF, Peng ZX, Ding L and Peng YR. Baishouwu extract suppresses the development of hepatocellular carcinoma via TLR4/MyD88/NF-

kappaB pathway. Front Pharmacol 2019; 10: 389.
[6] Jing YY, Han ZP, Sun K, Zhang SS, Hou J, Liu Y, Li R, Gao L, Zhao X, Zhao QD, Wu MC and Wei LX. Toll-like receptor 4 signaling promotes epithelial-mesenchymal transition in human hepatocellular carcinoma induced by lipopolysaccharide. BMC Med 2012; 10: 98.
[7] Seki E, De Minicis S, Osterreicher CH, Kluwe J, Osawa Y, Brenner DA and Schwabe RF. TLR4 enhances TGF-beta signaling and hepatic fibrosis. Nat Med 2007; 13: 1324-1332.
[8] Yang J, Li M and Zheng QC. Emerging role of Toll-like receptor 4 in hepatocellular carcinoma. J Hepatocell Carcinoma 2015; 2: 11-17.
[9] Wang JP, Zhang Y, Wei X, Li J, Nan XP, Yu HT, Li Y, Wang PZ and Bai XF. Circulating Toll-like receptor (TLR) 2, TLR4, and regulatory T cells in patients with chronic hepatitis C. APMIS 2010; 118: 261-270.
[10] Wei XQ, Guo YW, Liu JJ, Wen ZF, Yang SJ and Yao JL. The significance of Toll-like receptor 4 (TLR4) expression in patients with chronic hepatitis B. Clin Invest Med 2008; 31: E123-130.
[11] Seki E and Brenner DA. Toll-like receptors and adaptor molecules in liver disease: update. Hepatology 2008; 48: 322-335.
[12] Wanka L, Iqbal K and Schreiner PR. The lipophilic bullet hits the targets: medicinal chemistry of adamantane derivatives. Chem Rev 2013; 113: 3516-3604.
[13] Liu J, Obando D, Liao V, Lifa T and Codd R. The many faces of the adamantyl group in drug design. Eur J Med Chem 2011; 46: 1949-1963.
[14] Lamoureux G and Artavia G. Use of the adamantane structure in medicinal chemistry. Curr Med Chem 2010; 17: 2967-2978.
[15] Davies WL, Grunert RR, Haff RF, McGahen JW, Neumayer EM, Paulshock M, Watts JC, Wood TR, Hermann EC and Hoffmann CE. Antiviral activity of 1-adamantanamine (amantadine). Science 1964; 144: 862-863.
[16] Wingfield WL, Pollack D and Grunert RR. Therapeutic efficacy of amantadine HCl and rimantadine HCl in naturally occurring influenza A2 respiratory illness in man. N Engl J Med 1969; 281: 579-584.
[17] Balzarini J, Orzeszko-Krzesinska B, Maurin JK and Orzeszko A. Synthesis and anti-HIV studies of 2- and 3-adamantyl-substituted thiazolidin-4-ones. Eur J Med Chem 2009; 44: 303-311.
[18] El-Emam AA, Al-Deeb OA, Al-Omar M and Lehmann J. Synthesis, antimicrobial, and anti-HIV-1 activity of certain 5-(1-adamantyl)-2-substituted thio-1,3,4-oxadiazoles and 5-(1-adamantyl)-3-substituted aminomethyl-1,3,4-oxadiazoline-2-thiones. Bioorg Med Chem 2004; 12: 5107-5113.
[19] Rosenthal KS, Sokol MS, Ingram RL, Subramanian R and Fort RC. Tromantadine: inhibitor of early and late events in herpes simplex virus replication. Antimicrob Agents Chemother 1982; 22: 1031-1036.
[20] Han T, Goralski M, Capota E, Padrick SB, Kim J, Xie Y and Nijhawan D. The antitumor toxin CD437 is a direct inhibitor of DNA polymerase alpha. Nat Chem Biol 2016; 12: 511-515.
[21] Sun SY, Yue P, Chen X, Hong WK and Lotan R. The synthetic retinoid CD437 selectively induces apoptosis in human lung cancer cells while sparing normal human lung epithelial cells. Cancer Res 2002; 62: 2430-2436.
[22] Lorenzo P, Alvarez R, Ortiz MA, Alvarez S, Piedrafita FJ and de Lera AR. Inhibition of IkappaB kinase-beta and anticancer activities of novel chalcone adamantyl arotinoids. J Med Chem 2008; 51: 5431-5440.
[23] Lorenzo P, Ortiz MA, Alvarez R, Piedrafita FJ and de Lera AR. Adamantyl arotinoids that inhibit IkappaB kinase alpha and IkappaB kinase beta. ChemMedChem 2013; 8: 1184-1198.
[24] Britten CD, Garrett-Mayer E, Chin SH, Shirai K, Ogretmen B, Bentz TA, Brisendine A, Anderton K, Cusack SL, Maines LW, Zhuang Y, Smith CD and Thomas MB. A phase I study of ABC294640, a first-in-class sphingosine kinase-2 inhibitor, in patients with advanced solid tumors. Clin Cancer Res 2017; 23: 4642-4650.
[25] McNaughton M, Pitman M, Pitson SM, Pyne NJ and Pyne S. Proteasomal degradation of sphingosine kinase 1 and inhibition of dihydroceramide desaturase by the sphingosine kinase inhibitors, SKi or ABC294640, induces growth arrest in androgen-independent LNCaP-AI prostate cancer cells. Oncotarget 2016; 7: 16663-16675.
[26] Burmistrov V, Morisseau C, Harris TR, Butov G and Hammock BD. Effects of adamantane alterations on soluble epoxide hydrolase inhibition potency, physical properties and metabolic stability. Bioorg Chem 2018; 76: 510-527.
[27] Burmistrov V, Morisseau C, Pitushkin D, Karlov D, Fayzullin RR, Butov GM and Hammock BD. Adamantyl thioureas as soluble epoxide hydrolase inhibitors. Bioorg Med Chem Lett 2018; 28: 2302-2313.
[28] Butov GM, Burmistrov VV, Danilov DV, Pitushkin DA, Morisseau C and Hammock BD. Synthesis of adamantyl-containing 1,3-disubstituted diureas and thioureas, efficient targeted inhibitors of human soluble epoxide hydrolase. Russian Chemical Bulletin 2016; 64: 1569-1575.
[29] Wang W, Yang J, Zhang J, Wang Y, Hwang SH, Qi W, Wan D, Kim D, Sun J, Sanidad KZ, Yang H, Park Y, Liu JY, Zhao X, Zheng X, Liu Z, Hammock BD and Zhang G. Lipidomic profiling reveals soluble epoxide hydrolase as a therapeutic target of obesity-induced colonic inflam-

mation. Proc Natl Acad Sci U S A 2018; 115: 5283-5288.
[30] Zhang CH, Zheng L, Gui L, Lin JY, Zhu YM, Deng WS and Luo M. Soluble epoxide hydrolase inhibition with t-TUCB alleviates liver fibrosis and portal pressure in carbon tetrachloride-induced cirrhosis in rats. Clin Res Hepatol Gastroenterol 2017; 42: 118-125.
[31] Zhang G, Panigrahy D, Hwang SH, Yang J, Mahakian LM, Wettersten HI, Liu JY, Wang Y, Ingham ES, Tam S, Kieran MW, Weiss RH, Ferrara KW and Hammock BD. Dual inhibition of cyclooxygenase-2 and soluble epoxide hydrolase synergistically suppresses primary tumor growth and metastasis. Proc Natl Acad Sci U S A 2014; 111: 11127-11132.
[32] Al-Wahaibi LH, Hassan HM, Abo-Kamar AM, Ghabbour HA and El-Emam AA. Adamantane-isothiourea hybrid derivatives: synthesis, characterization, in vitro antimicrobial, and in vivo hypoglycemic activities. Molecules 2017; 22: 710
[33] Al-Mutairi AA, Al-Alshaikh MA, Al-Omary FAM, Hassan HM, El-Mahdy AM and El-Emam AA. Synthesis, antimicrobial, and anti-proliferative activities of novel 4-(Adamantan-1-yl)-1-arylidene-3-thiosemicarbazides, 4-Arylmethyl N'-(Adamantan-1-yl)piperidine-1-carbothioimidates, and related derivatives. Molecules 2019; 24: 4308.
[34] Koronkiewicz M, Romiszewska A, Chilmonczyk Z and Kazimierczuk Z. New benzimidazole-derived isothioureas as potential antileukemic agents--studies in vitro. Med Chem 2015; 11: 364-372.
[35] Nicholson A, Perry JD, James AL, Stanforth SP, Carnell S, Wilkinson K, Anjam Khan CM, De Soyza A and Gould FK. In vitro activity of S-(3,4-dichlorobenzyl)isothiourea hydrochloride and novel structurally related compounds against multidrug-resistant bacteria, including Pseudomonas aeruginosa and Burkholderia cepacia complex. Int J Antimicrob Agents 2012; 39: 27-32.
[36] Shearer BG, Lee S, Oplinger JA, Frick LW, Garvey EP and Furfine ES. Substituted N-phenylisothioureas: potent inhibitors of human nitric oxide synthase with neuronal isoform selectivity. J Med Chem 1997; 40: 1901-1905.
[37] Thoma G, Streiff MB, Kovarik J, Glickman F, Wagner T, Beerli C and Zerwes HG. Orally bioavailable isothioureas block function of the chemokine receptor CXCR4 in vitro and in vivo. J Med Chem 2008; 51: 7915-7920.
[38] Berridge MV and Tan AS. Characterization of the cellular reduction of 3-(4,5-dimethylthiazol-2-yl)-2,5-diphenyltetrazolium bromide (MTT): subcellular localization, substrate dependence, and involvement of mitochondrial electron transport in MTT reduction. Arch Biochem Biophys 1993; 303: 474-482.
[39] Mosmann T. Rapid colorimetric assay for cellular growth and survival: application to proliferation and cytotoxicity assays. J Immunol Methods 1983; 65: 55-63.
[40] Elmansi AM, El-Karef AA, Shishtawy M and Eissa LA. Hepatoprotective effect of curcumin on hepatocellular carcinoma through autophagic and apoptic pathways. Ann Hepatol 2017; 16: 607-618.
[41] Helmy SA, El-Mesery M, El-Karef A, Eissa LA and El Gayar AM. Chloroquine upregulates TRAIL/TRAILR2 expression and potentiates doxorubicin anti-tumor activity in thioacetamide-induced hepatocellular carcinoma model. Chem Biol Interact 2017; 279: 84-94.
[42] Daher S, Massarwa M, Benson AA and Khoury T. Current and future treatment of hepatocellular carcinoma: an updated comprehensive review. J Clin Transl Hepatol 2018; 6: 69-78.
[43] Becker FF. Thioacetamide hepatocarcinogenesis. J Natl Cancer Inst 1983; 71: 553-558.
[44] Gervasi PG, Longo V, Marzano M, Saviozzi M and Malvaldi G. Chronic liver injury by thioacetamide and promotion of hepatic carcinogenesis. J Cancer Res Clin Oncol 1989; 115: 29-35.
[45] Yeo W, Mok TS, Zee B, Leung TW, Lai PB, Lau WY, Koh J, Mo FK, Yu SC, Chan AT, Hui P, Ma B, Lam KC, Ho WM, Wong HT, Tang A and Johnson PJ. A randomized phase III study of doxorubicin versus cisplatin/interferon alpha-2b/doxorubicin/fluorouracil (PIAF) combination chemotherapy for unresectable hepatocellular carcinoma. J Natl Cancer Inst 2005; 97: 1532-1538.
[46] Yuan JN, Chao Y, Lee WP, Li CP, Lee RC, Chang FY, Yen SH, Lee SD and Whang-Peng J. Chemotherapy with etoposide, doxorubicin, cisplatin, 5-fluorouracil, and leucovorin for patients with advanced hepatocellular carcinoma. Med Oncol 2008; 25: 201-206.
[47] Tacar O, Sriamornsak P and Dass CR. Doxorubicin: an update on anticancer molecular action, toxicity and novel drug delivery systems. J Pharm Pharmacol 2013; 65: 157-170.
[48] Abou-Alfa GK, Johnson P, Knox JJ, Capanu M, Davidenko I, Lacava J, Leung T, Gansukh B and Saltz LB. Doxorubicin plus sorafenib vs doxorubicin alone in patients with advanced hepatocellular carcinoma: a randomized trial. JAMA 2010; 304: 2154-2160.
[49] Chang TS, Wu YC, Tung SY, Wei KL, Hsieh YY, Huang HC, Chen WM, Shen CH, Lu CH, Wu CS, Tsai YH and Huang YH. Alpha-fetoprotein measurement benefits hepatocellular carcinoma surveillance in patients with cirrhosis. Am J Gastroenterol 2015; 110: 836-844; quiz 845.
[50] Aly SM, Fetaih HA, Hassanin AAI, Abomughaid MM and Ismail AA. Protective effects of garlic and cinnamon oils on hepatocellular carcino-

ma in albino rats. Anal Cell Pathol (Amst) 2019; 2019: 9895485.
[51] Arand M, Grant DF, Beetham JK, Friedberg T, Oesch F and Hammock BD. Sequence similarity of mammalian epoxide hydrolases to the bacterial haloalkane dehalogenase and other related proteins. Implication for the potential catalytic mechanism of enzymatic epoxide hydrolysis. FEBS Lett 1994; 338: 251-256.
[52] Spector AA, Fang X, Snyder GD and Weintraub NL. Epoxyeicosatrienoic acids (EETs): metabolism and biochemical function. Prog Lipid Res 2004; 43: 55-90.
[53] Biliktu M, Senol SP, Temiz-Resitoglu M, Guden DS, Horat MF, Sahan-Firat S, Sevim S and Tunctan B. Pharmacological inhibition of soluble epoxide hydrolase attenuates chronic experimental autoimmune encephalomyelitis by modulating inflammatory and anti-inflammatory pathways in an inflammasome-dependent and -independent manner. Inflammopharmacology 2020; 28: 1509-1524.
[54] Liu JY, Park SH, Morisseau C, Hwang SH, Hammock BD and Weiss RH. Sorafenib has soluble epoxide hydrolase inhibitory activity, which contributes to its effect profile in vivo. Mol Cancer Ther 2009; 8: 2193-2203.
[55] Ding YF, Wu ZH, Wei YJ, Shu L and Peng YR. Hepatic inflammation-fibrosis-cancer axis in the rat hepatocellular carcinoma induced by diethylnitrosamine. J Cancer Res Clin Oncol 2017; 143: 821-834.
[56] Song IJ, Yang YM, Inokuchi-Shimizu S, Roh YS, Yang L and Seki E. The contribution of toll-like receptor signaling to the development of liver fibrosis and cancer in hepatocyte-specific TAK1-deleted mice. Int J Cancer 2017; 142: 81-91.
[57] Wang L, Zhu R, Huang Z, Li H and Zhu H. Lipopolysaccharide-induced toll-like receptor 4 signaling in cancer cells promotes cell survival and proliferation in hepatocellular carcinoma. Dig Dis Sci 2013; 58: 2223-2236.
[58] Cheng Y, Luo R, Zheng H, Wang B, Liu Y, Liu D, Chen J, Xu W, Li A and Zhu Y. Synergistic antitumor efficacy of sorafenib and fluvastatin in hepatocellular carcinoma. Oncotarget 2017; 8: 23265-23276.
[59] Kang Y, Su G, Sun J and Zhang Y. Activation of the TLR4/MyD88 signaling pathway contributes to the development of human hepatocellular carcinoma via upregulation of IL-23 and IL-17A. Oncol Lett 2018; 15: 9647-9654.
[60] Li JJ, Luo J, Lu JN, Liang XN, Luo YH, Liu YR, Yang J, Ding H, Qin GH, Yang LH, Dang YW, Yang H and Chen G. Relationship between TRAF6 and deterioration of HCC: an immunohistochemical and in vitro study. Cancer Cell Int 2016; 16: 76.
[61] Berasain C, Castillo J, Perugorria MJ, Latasa MU, Prieto J and Avila MA. Inflammation and liver cancer: new molecular links. Ann N Y Acad Sci 2009; 1155: 206-221.
[62] Pikarsky E, Porat RM, Stein I, Abramovitch R, Amit S, Kasem S, Gutkovich-Pyest E, Urieli-Shoval S, Galun E and Ben-Neriah Y. NF-kappaB functions as a tumour promoter in inflammation-associated cancer. Nature 2004; 431: 461-466.
[63] Capece D, Fischietti M, Verzella D, Gaggiano A, Cicciarelli G, Tessitore A, Zazzeroni F and Alesse E. The inflammatory microenvironment in hepatocellular carcinoma: a pivotal role for tumor-associated macrophages. Biomed Res Int 2013; 2013: 187204.
[64] Park EJ, Lee JH, Yu GY, He G, Ali SR, Holzer RG, Osterreicher CH, Takahashi H and Karin M. Dietary and genetic obesity promote liver inflammation and tumorigenesis by enhancing IL-6 and TNF expression. Cell 2010; 140: 197-208.
[65] Voronov E, Shouval DS, Krelin Y, Cagnano E, Benharroch D, Iwakura Y, Dinarello CA and Apte RN. IL-1 is required for tumor invasiveness and angiogenesis. Proc Natl Acad Sci U S A 2003; 100: 2645-2650.
[66] Scharenberg MA, Pippenger BE, Sack R, Zingg D, Ferralli J, Schenk S, Martin I and Chiquet-Ehrismann R. TGF-beta-induced differentiation into myofibroblasts involves specific regulation of two MKL1 isoforms. J Cell Sci 2014; 127: 1079-1091.
[67] Giannelli G, Villa E and Lahn M. Transforming growth factor-beta as a therapeutic target in hepatocellular carcinoma. Cancer Res 2014; 74: 1890-1894.
[68] Shang N, Bank T, Ding X, Breslin P, Li J, Shi B and Qiu W. Caspase-3 suppresses diethylnitrosamine-induced hepatocyte death, compensatory proliferation and hepatocarcinogenesis through inhibiting p38 activation. Cell Death Dis 2018; 9: 558.

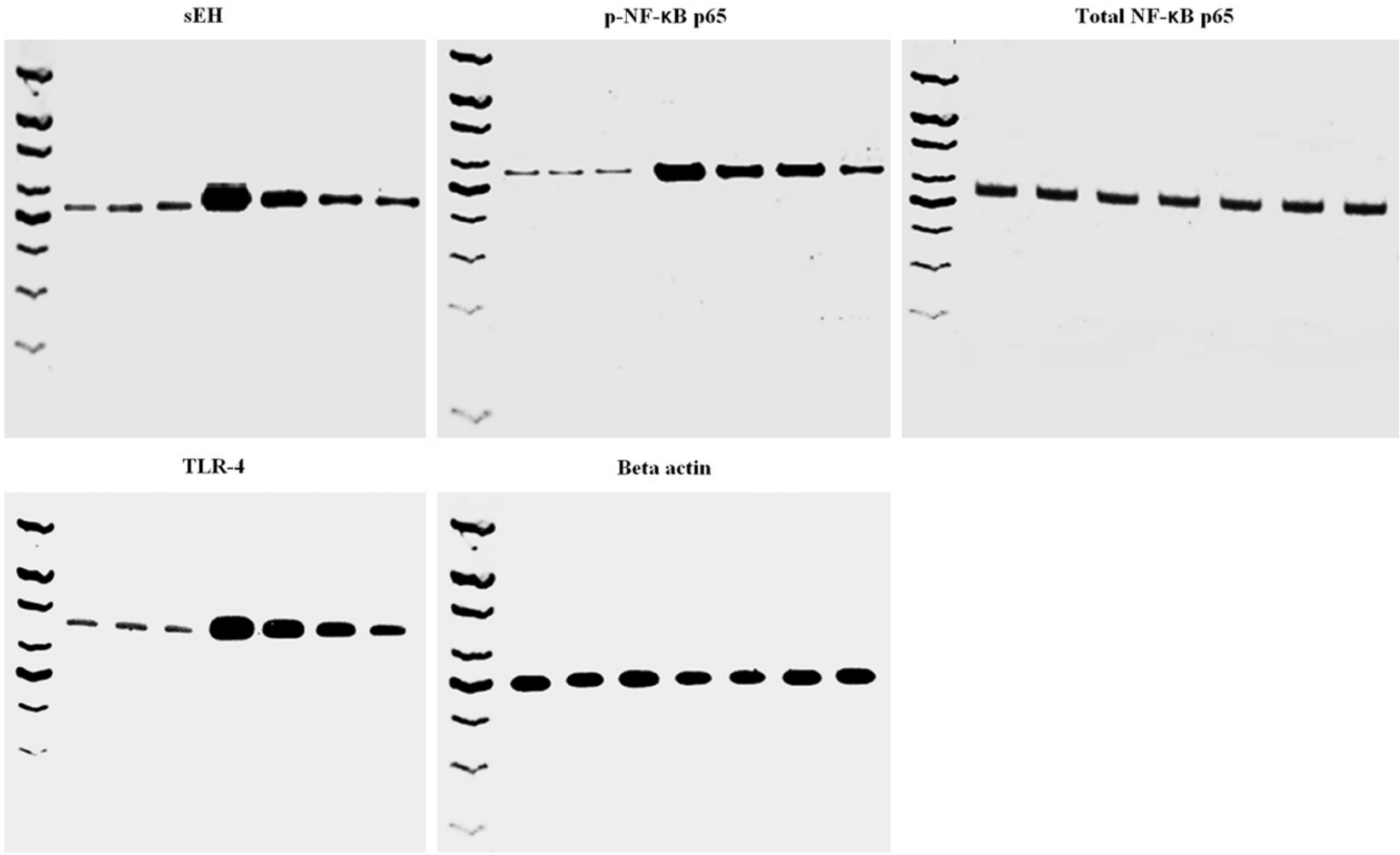

Figure S1. Original Blots of **Figure 8A**.